Imaging Science in Dentistry 2023; 53: 61-7
https://doi.org/10.5624/isd.20220186

A novel method of objectively detecting tooth ankylosis using cone-beam computed tomography: A laboratory study

Luciano Augusto Cano Martins[1], Danieli Moura Brasil[1], Deborah Queiroz Freitas[1], Matheus L Oliveira[1,*]

[1]*Division of Oral Radiology, Department of Oral Diagnosis, Piracicaba Dental School, University of Campinas, Piracicaba, SP, Brazil*

ABSTRACT

Purpose: The aim of this study was to objectively detect simulated tooth ankylosis using a novel method involving cone-beam computed tomography (CBCT).

Materials and Methods: Tooth ankylosis was simulated in single-rooted human permanent teeth, and CBCT scans were acquired at different current levels (5, 6.3, and 8 mA) and voxel sizes (0.08, 0.125, and 0.2). In axial reconstructions, a line of interest was perpendicularly placed over the periodontal ligament space of 21 ankylosed and 21 non-ankylosed regions, and the CBCT grey values of all voxels along the line of interest were plotted against their corresponding X-coordinates through a line graph to generate a profile. The image contrast was increased by 30% and 60% and the profile assessment was repeated. The internal area of the resulting parabolas was obtained from all images and compared between ankylosed and non-ankylosed regions under different contrast enhancement conditions, voxel sizes, and mA levels using multi-way analysis of variance with the Tukey *post hoc* test ($\alpha = 0.05$).

Results: The internal area of the parabolas of all non-ankylosed regions was significantly higher than that of the ankylosed regions ($P < 0.05$). Contrast enhancement led to a significantly greater internal area of the parabolas of non-ankylosed regions ($P < 0.05$). Overall, voxel size and mA did not significantly influence the internal area of the parabolas ($P > 0.05$).

Conclusion: The proposed novel method revealed a relevant degree of applicability in the detection of simulated tooth ankylosis; increased image contrast led to greater detectability. ***(Imaging Sci Dent 2023; 53: 61-7)***

KEY WORDS: Periodontal Ligament; Cone-Beam Computed Tomography; Diagnostic Imaging; Imaging, Three-Dimensional

Introduction

Tooth ankylosis is clinically suspected when the affected tooth is infra-occluded or impacted and does not respond to orthodontic forces. Histologically, it is defined as the fusion of the root surface (either cementum or dentin) with the adjacent alveolar bone, which leads to partial or complete obliteration of the periodontal ligament (PDL) space, thus making imaging examinations a relevant complementary tool.[1] Previous studies have demonstrated that cone-beam computed tomography (CBCT) more accurately represents the PDL space than 2-dimensional radiography. However, the diagnosis of tooth ankylosis remains challenging, mostly because of the discrete aspect of this condition in the face of the spatial resolution of contemporary CBCT machines.[2-6] A CBCT volumetric dataset is composed of cuboidal volume elements, also referred to as voxels, which contain specific grey values according to the linear X-ray attenuation coefficient of the corresponding tissues.[7] Inconsistences in the accuracy of CBCT grey values have been reported and attributed to exposure parameters, reconstruction algorithms, artefact formation, technological factors, and anatomical location.[8] However, although it is not appropriate to assume

This study was financed in part by the Coordenação de Aperfeiçoamento de Pessoal de Nível Superior - Brazil (CAPES) - Finance Code 001.
Received October 18, 2022; Revised December 12, 2022; Accepted December 14, 2022
Published online January 11, 2023
*Correspondence to : Prof. Matheus L Oliveira
Division of Oral Radiology, Department of Oral Diagnosis, Piracicaba Dental School, University of Campinas. Piracicaba Dental School, Av. Limeira, 901, Piracicaba, SP 13414-903, Brazil
Tel) 55-19-2106-5327, E-mail) luciano_cano@hotmail.com

Copyright ⓒ 2023 by Korean Academy of Oral and Maxillofacial Radiology
This is an Open Access article distributed under the terms of the Creative Commons Attribution Non-Commercial License (http://creativecommons.org/licenses/by-nc/3.0) which permits unrestricted non-commercial use, distribution, and reproduction in any medium, provided the original work is properly cited.

specific physical features of the object of interest based on any given CBCT-derived grey value, a strong linear relationship between grey values and object density has been observed.[9-12]

A recent study has objectively quantified mean grey values of ankylosed regions of unerupted or partially erupted teeth in patients' CBCT scans and observed higher grey values in ankylosed regions.[10] This finding reveals the potential ability of CBCT grey values for that diagnostic purpose; however, the mean grey values of the PDL space and adjacent hard tissues may be strongly influenced by slightly different positioning of the region of interest. Alternatively, another quantitative approach to visually interpret CBCT grey values is by plotting them against their corresponding spatial location (X-coordinate) to display a 2-dimensional graph, also referred to as a plot profile. Accordingly, the resulting profile of the grey values of a short straight line placed perpendicularly and centrally to a PDL space under normal conditions is a parabola, such that the vertex of the parabola represents the centre of the PDL space, and the bilateral ascending curves represent the alveolar bone and root surface.

The determination of an indisputable gold standard of tooth ankylosis in clinical studies with human subjects is difficult and debatable. In this context, *in vitro* studies allow for a highly controlled environment with a clear gold standard and a larger sample size. Considering the clinical importance of accurately detecting tooth ankylosis, the aim of this study was to evaluate simulated tooth ankylosis quantitatively and objectively, using a novel method developed from the profile of grey values in CBCT examinations with different contrast conditions, voxel sizes, and mA.

Materials and Methods

Ethical aspects and sample size

This *in vitro* study was reviewed and approved by the local Research Ethics Committee (protocol# 3.927.561) and complied with the Helsinki Declaration.

A pilot study was performed using 10 experimental units for each experimental group to test the method and calculate the sample size. Based on the minimum differences between the experimental groups and the standard deviation of each experimental group, a sample size of 21 ankylosed regions was found to meet statistical criteria with a test power of 95% and a significance level of 5%.

Tooth ankylosis simulation and CBCT acquisition

In total, 30 single-rooted mandibular permanent teeth including canines and premolars were distributed in 10 phantoms of 3 teeth each. The roots of all teeth were coated with a 0.25-mm-thick layer of wax (Lysanda, São Paulo, Brazil) to simulate the PDL space by submerging each root in melted wax, confirming the desired width with a periodontal probe, and, if needed, removing wax with a Lecron carver. A portion of wax measuring 2 × 2 mm or 4 × 2 mm (height × width) was carefully and completely removed from half of the sample (n = 15) following a previously published methodology.[6] The wax removal site was randomly distributed among the 3 root thirds (cervical, middle, or apical) and 4 root surfaces (buccal, lingual, mesial, or distal) to simulate different clinical situations. After wax removal, the teeth were inserted into a fluid mixture of stone plaster type 3 (Asfer, São Caetano do Sul, São Paulo, Brazil) and ground rice in a volume proportion of 2 : 1 to visually simulate trabecular bone. Tooth ankylosis simulation was confirmed with micro-CT images revealing the penetration of the plaster mixture into the wax defect and a homogeneous thickness of wax representing the PDL space.

All phantoms were inserted into a polypropylene container (12 × 10 cm) filled with water to simulate soft-tissue attenuation, centred in a 5 × 5 cm field of view, and individually scanned with the CBCT device OP300 Maxio (Instrumentarium, Tuusula, Finland) adjusted with 90 kVp and 9 protocols varying the 3 currents (5, 6.3, and 8 mA) and 3 voxel sizes (0.08, 0.125, and 0.2 mm).

Image evaluation

To determine the axial reconstruction to be analysed, the examiner considered clear visualisation of the simulated tooth ankylosis and the normal periodontal ligament space. In selected CBCT axial reconstructions and using the ImageJ software (NIH, Bethesda, MD, USA), a straight line of interest (LOI) measuring 1.00 mm in length was perpendicularly centred over the PDL space of 21 ankylosed (Fig. 1A) and 21 non-ankylosed (Fig. 1B) regions such that the LOI equally extended and bilaterally from the centre of the PDL space to bone and dentin. Because the number of ankylosed and non-ankylosed teeth was 15, 6 teeth in each experimental group had 2 LOIs to reach the total of 21 LOIs per group. To avoid a potential source of bias in the placement of 2 LOIs in the same ankylosed teeth, only those with larger wax defects (2 × 4 mm) were selected so that the LOIs were not excessively close to each other. The CBCT grey values along the LOIs and their corresponding X-coordinates were collected.

Additionally, 2 oral radiologists, in consensus, defined 2 high-contrast enhancement levels and applied them to all original images: C1 (30% increase in contrast; the minimum

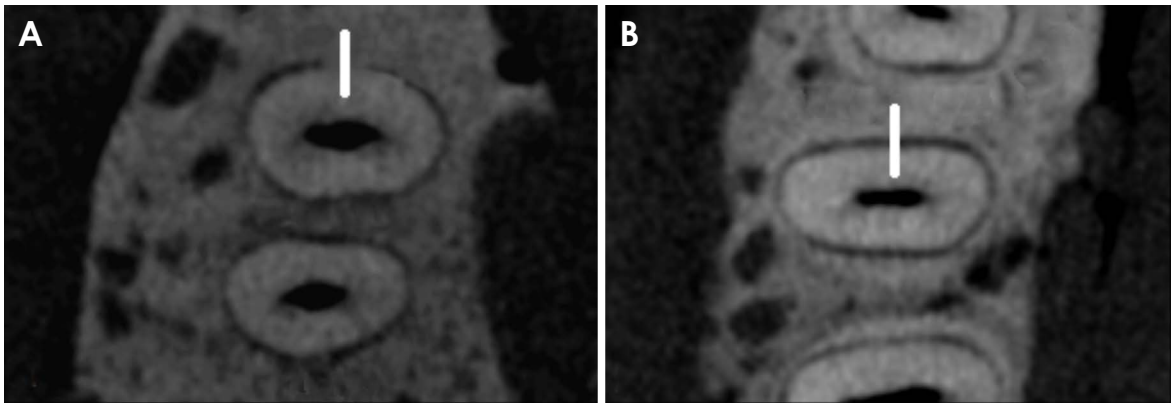

Fig. 1. Representative cropped cone-beam computed tomographic axial reconstructions with the line of interest (white solid line) placed over an ankylosed region (A) and a non-ankylosed region (B).

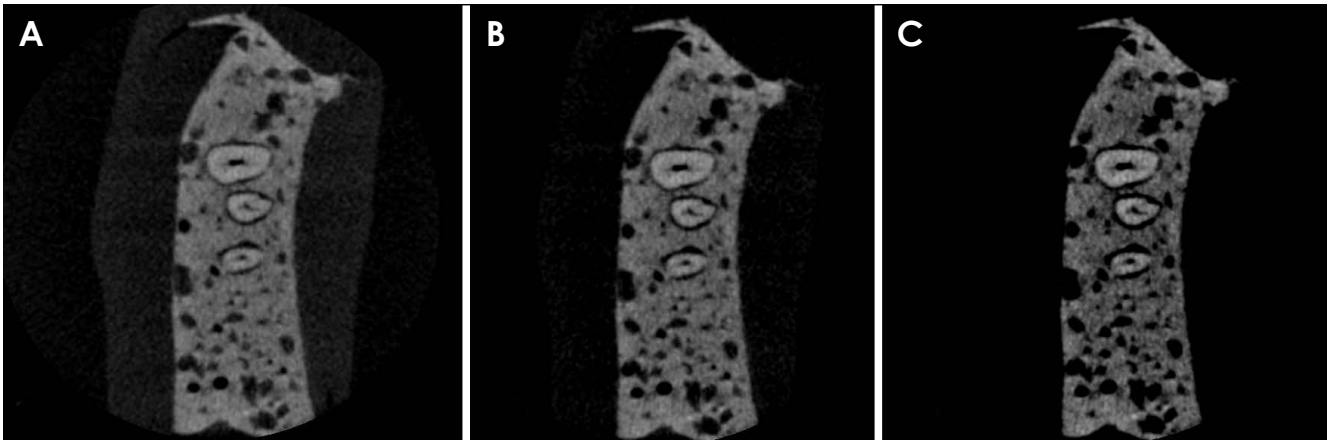

Fig. 2. Representative cone-beam computed tomographic axial reconstructions of the same imaging phantom at 3 contrast enhancement conditions. A. Original. B. 30% contrast increase (C1). C. 60% contrast increase (C2).

and maximum grey values were, respectively, 21 and 234) and C2 (60% increase in contrast as the highest clinically acceptable level of contrast for the visualisation of the PDL space; the minimum and maximum grey values were, respectively, 51 and 204) (Fig. 2). Similar to the original images, CBCT grey values and their corresponding X-coordinates were obtained from LOIs placed over the same regions of CBCT images at C1 and C2. To ensure that the LOIs had the exact same location for the same region under different contrast enhancement conditions, the ROI manager in ImageJ was used. All collected data were imported to GeoGebra, an open-source application (http://www.geogebra.org), and the CBCT grey values were plotted against their X-coordinates to generate a 2-dimensional line graph (Fig. 3). The internal area of the resulting parabolas, in square units of area, was measured for each LOI and contrast enhancement condition, totalling 1134 internal areas [(21 ankylosed regions + 21 non-ankylosed regions) × 3 contrast enhancement conditions × 3 voxel sizes × 3 currents].

After 30 days of the completion of image evaluation, half of the sample, equally distributed among the experimental groups, was re-evaluated to assess intra-examiner agreement.

Statistical analysis

In SPSS version 23.0 (IBM Corp., Armonk, NY, USA), multi-way analysis of variance with the Tukey *post hoc* test was used to compare the internal area of the parabola (outcome variable) between ankylosed and non-ankylosed regions under different contrast enhancement conditions, voxel sizes, and mA settings at a significance level of 5% ($\alpha = 0.05$). Intra-examiner agreement was evaluated using the intra-class correlation coefficient.

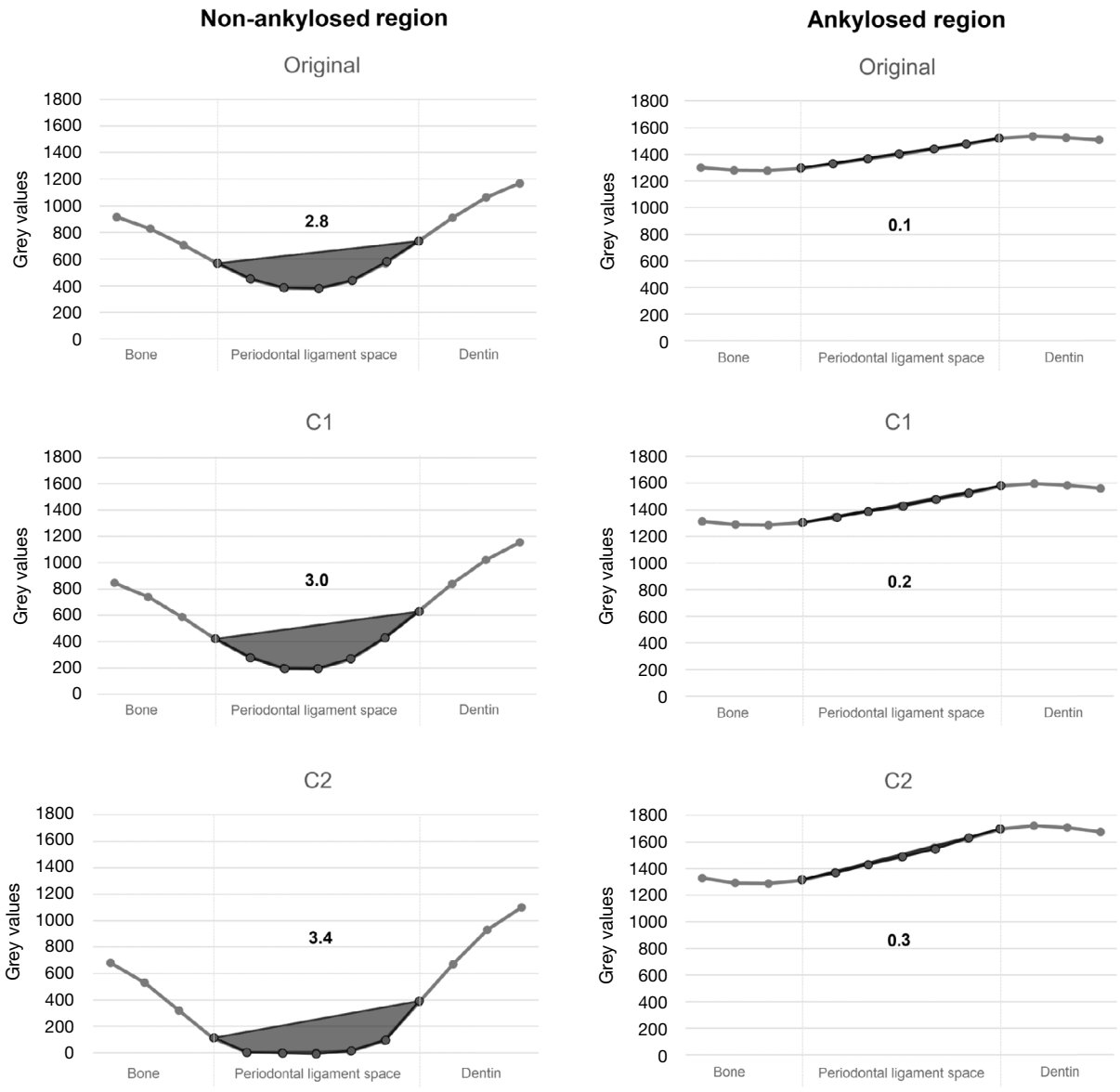

Fig. 3. Line graphs of the profile of cone-beam computed tomographic grey values of a line of interest placed over a representative non-ankylosed and ankylosed region under 3 contrast enhancement conditions (original, C1, and C2). The bold number in the centre of each graph represents the internal area of the parabola (shaded zone) in square units of area.

Results

As shown in Table 1, the proposed novel method developed from the profile of CBCT grey values revealed interesting applicability in the detection of simulated tooth ankylosis, as the internal area of the parabolas of all non-ankylosed regions was significantly higher than that of the ankylosed regions within the same mA level, voxel size, and contrast enhancement conditions ($P<0.05$). Furthermore, contrast enhancement improved the detection of non-ankylosed regions with images under C2, revealing significantly higher values of the internal area of the parabolas than those under C1, which led to significantly greater values than the original images ($P<0.05$).

Overall, the voxel size and mA did not significantly influence the internal area of the parabolas ($P>0.05$), with two inconsistent exceptions: 1) the 0.08-mm voxel size in non-ankylosed regions at 6.3 mA and C1 and C2 contrast enhancement conditions showed significantly greater values than those of 0.125- and 0.2-mm voxel sizes ($P<0.05$), and 2) the 8 mA setting in non-ankylosed regions at 0.08-mm voxel size and C1 and C2 contrast enhancement conditions

Table 1. Mean values (standard deviation) of the internal area of the parabolas of non-ankylosed and ankylosed regions (in cm^2) at different contrast enhancement conditions, voxel sizes, and mA levels

Current	Voxel size (mm)	Contrast condition	Non-ankylosed region	Ankylosed region*
5 mA	0.08	Original	2.17 (0.67) c	0.44 (0.39)
		Contrast 1	4.74 (1.48) b	0.98 (0.82)
		Contrast 2	6.31 (1.53) a	1.65 (1.43)
	0.125	Original	1.61 (0.74) c	0.34 (0.35)
		Contrast 1	3.19 (1.61) b	0.84 (0.76)
		Contrast 2	4.40 (2.21) a	1.39 (1.24)
	0.2	Original	1.47 (0.68) c	0.54 (0.49)
		Contrast 1	2.95 (1.13) b	1.17 (1.07)
		Contrast 2	4.40 (1.69) a	1.90 (1.55)
6.3 mA	0.08	Original	1.94 (0.88) c	0.57 (0.39)
		Contrast 1	4.19 (2.01) b †	1.22 (0.74)
		Contrast 2	5.79 (2.05) a †	2.02 (1.30)
	0.125	Original	1.38 (1.26) c	0.41 (0.32)
		Contrast 1	2.40 (1.24) b	0.80 (0.60)
		Contrast 2	3.51 (1.64) a	1.38 (1.01)
	0.2	Original	1.17 (0.67) c	0.30 (0.24)
		Contrast 1	2.51 (1.04) b	0.65 (0.46)
		Contrast 2	3.97 (1.68) a	1.12 (0.73)
8 mA	0.08	Original	1.15 (0.52) c	0.43 (0.43)
		Contrast 1	2.34 (1.07) b ǂ	0.86 (0.84)
		Contrast 2	3.53 (1.90) a ǂ	1.26 (1.02)
	0.125	Original	1.42 (0.54) c	0.52 (0.59)
		Contrast 1	2.96 (1.20) b	0.95 (0.63)
		Contrast 2	4.61 (2.16) a	1.44 (0.85)
	0.2	Original	0.94 (0.64) c	0.15 (0.15)
		Contrast 1	2.21 (0.89) b	0.45 (0.35)
		Contrast 2	3.60 (1.52) a	0.88 (0.61)

*: significantly different from non-ankylosed regions irrespective of the mA level, voxel size, and contrast enhancement conditions. Different lowercase letters show a significant difference between contrast enhancement conditions, within the same mA and voxel size. †: significantly different from 0.125- and 0.2-mm voxel sizes under the same mA and contrast conditions. ǂ: significantly different from 5- and 6.3-mA currents under the same voxel size and contrast conditions

showed significantly lower values than those at the 5 and 6.3 mA settings ($P < 0.05$). The intra-class correlation coefficient value was excellent (0.9180).

Discussion

Despite the well-known advantages of CBCT for multiple diagnostic tasks in dentistry, the diagnosis of tooth ankylosis in clinical practice remains a challenge because of the discrete dimensions and limited access to the affected structures.[6] The inaccuracy of CBCT grey values in the representation of tissue density has been extensively described in the scientific literature.[8] Although absolute CBCT grey values, unlike CT-derived Hounsfield units, cannot be used for quantitative analysis of bone quality, they have demonstrated a strong linear correlation with the linear X-ray attenuation coefficient of tissues; accordingly, higher CBCT grey values can be expected from hard tissues and lower CBCT grey values can be expected from soft tissues.[9-12]

Because the PDL space is filled with soft tissue, the corresponding grey values are lower than those from the adjacent hard tissues, as was observed in the non-ankylosed regions

of this study, which led to a significantly greater internal area of the resulting parabolas. In the present study, the profile of CBCT grey values was plotted along a short straight line placed perpendicularly to the PDL space, from bone to dentin, against their corresponding X-coordinates to display a 2-dimensional graph. When ankylosis was simulated, because the PDL space was missing and the corresponding region was filled with bone-like material, a parabola was not generated because of the relative similarity of the CBCT grey values along the line of interest. This finding reveals that the novel objective analysis proposed in the present study was useful in the detection of simulated ankylosed regions and strongly suggests that, after clinical validation, this may possibly be translated to clinical practice. A previous clinical study has already found higher grey values in square regions of interest placed over regions of suspected ankylosis; however, because of the microscopic nature of the PDL space, associated with the fact that the outcome of a planar region of interest is an average of the grey values of multiple pixels, this method is susceptible to the proportion between hyperdense and hypodense structures and leaves room for further methods like the one proposed herein.[10]

Depending on the diagnostic task, CBCT grey values may be partially enhanced by brightness and contrast adjustments, thus favouring the visualisation of anatomical structures and reduction of artefacts.[13] This study tested 2 different contrast enhancement conditions (C1 and C2) by increasing image contrast to better visualise the PDL space by 30 and 60%, respectively. Both conditions increased the internal area of the parabola of non-ankylosed regions, which means that grey values of the PDL space were more differentiated from adjacent bone and dental root surfaces. For that reason, the authors strongly suggest increasing the contrast when using the present objective method for better representation of the PDL space.

When tooth ankylosis is suspected, the fusion of bone with the root surface is expected to lead to partial visualisation of the PDL space in CBCT; however, a previous study demonstrated that the CBCT-based subjective diagnosis is very challenging.[5,6] When compared to intraoral radiography, CBCT examinations obtained with small voxel sizes (0.075-0.2 mm) provide better visualisation of the PDL space, which increases spatial resolution and is useful for better visualising thin structures.[14-16] The normal width of the PDL space ranges from 0.15 to 0.38 mm; nevertheless, it may be reduced when the cementum layer is injured or with the aging process.[17,18] In this study, a PDL space of 0.25 mm was simulated as being within the normal range, and this was greater than the tested voxel sizes (0.08, 0.125, and 0.2 mm).

Grey values in CBCT may be influenced by many factors such as exposure parameters, image formation, reconstruction algorithms, artefact formation, technological factors, and anatomical location.[9] In general, current (expressed in units of mA) determines the number of electrons available in the X-ray tube that will be transformed into X-ray photons; a higher current leads to an increased signal-to-noise ratio, which is expected to improve image quality, but also increases the radiation dose delivered to the patient. This study tested 3 currents - 5, 6.3, and 8 mA - which, in general, did not affect the detection of tooth ankylosis; this suggests that the reduction of mA should be preferred to comply with radiation protection principles.

It is important to highlight that the present laboratory study was not able to reproduce possible involuntary movements of patients, which can be considered a limitation since it may have resulted in an overestimation of the detection of tooth ankylosis due to the increased image sharpness. Depending on the magnitude of motion artefacts, structures may be seen with a double contour. In addition, the phantoms did not have highly attenuating materials such as gutta percha or metal inserts, which is a frequent condition in dentistry that could have negatively affected the objective analyses due to artefact formation.[19] Conversely, the *ex vivo* model with carefully simulated lesions of tooth ankylosis served as an unquestionable gold standard, making it possible to obtain repeated CBCT scans of the same specimen, which, for ethical reasons, would not have been possible with living patients. Further studies focused on the clinical application of the present method developed from the profile of CBCT grey values and the possible influence of high-density objects close to suspected ankylosed teeth are strongly encouraged.

The proposed novel method developed from the profile of CBCT grey values revealed a relevant degree of applicability in the detection of simulated tooth ankylosis irrespective of the contrast enhancement condition, voxel size, and mA level. Furthermore, increased image contrast led to greater detectability.

Conflicts of Interest: None

References

1. Eşian D, Bica CI, Stoica OE, Dako T, Vlasa A, Bud ES, et al. Prevalence and manifestations of dental ankylosis in primary molars using panoramic X-rays: a cross-sectional study. Child-

ren (Basel) 2022; 9: 1188.
2. Choi IG, Cortes AR, Arita ES, Georgetti MA. Comparison of conventional imaging techniques and CBCT for periodontal evaluation: a systematic review. Imaging Sci Dent 2018; 48: 79-86.
3. Tayman MA, Kamburoğlu K, Öztürk E, Küçük Ö. The accuracy of periapical radiography and cone beam computed tomography in measuring periodontal ligament space: ex vivo comparative micro-CT study. Aust Endod J 2020; 46: 365-73.
4. Patcas R, Müller L, Ullrich O, Peltomäki T. Accuracy of cone-beam computed tomography at different resolutions assessed on the bony covering of the mandibular anterior teeth. Am J Orthod Dentofac Orthop 2012; 141: 41-50.
5. Ducommun F, Bornstein MM, Bosshardt D, Katsaros C, Dula K. Diagnosis of tooth ankylosis using panoramic views, cone beam computed tomography, and histological data: a retrospective observational case series study. Eur J Orthod 2018; 40: 231-8.
6. Martins LA, Brasil DM, Dos Santos JC, Freitas DQ, Oliveira ML. Is the efficacy of cone beam computed tomography in the diagnosis of tooth ankylosis influenced by dose reduction protocols? Oral Surg Oral Med Oral Pathol Oral Radiol 2022; 135: 129-35.
7. Pauwels R, Araki K, Siewerdsen JH, Thongvigitmanee SS. Technical aspects of dental CBCT: state of the art. Dentomaxillofac Radiol 2015; 44: 20140224.
8. Pauwels R, Jacobs R, Singer SR, Mupparapu M. CBCT-based bone quality assessment: are Hounsfield units applicable? Dentomaxillofac Radiol 2015; 44: 20140238.
9. Oliveira ML, Freitas DQ, Ambrosano GM, Haiter-Neto F. Influence of exposure factors on the variability of CBCT voxel values: a phantom study. Dentomaxillofac Radiol 2014; 43: 20140128.
10. Rege IC, Botelho TL, Martins AF, Leles CR, Mendonça EF. Pixel gray measurement for the diagnosis of dental ankylosis in cone beam computed tomography images. Oral Surg Oral Med Oral Pathol Oral Radiol 2021; 131: 721-9.
11. Oliveira ML, Tosoni GM, Lindsey DH, Mendoza K, Tetradis S, Mallya SM. Assessment of CT numbers in limited and medium field-of-view scans taken using Accuitomo 170 and Veraview-epocs 3De cone-beam computed tomography scanners. Imaging Sci Dent 2014; 44: 279-85.
12. Oliveira ML, Tosoni GM, Lindsey DH, Mendoza K, Tetradis S, Mallya SM. Influence of anatomical location on CT numbers in cone beam computed tomography. Oral Surg Oral Med Oral Pathol Oral Radiol 2013; 115: 558-64.
13. Coelho-Silva F, Martins LA, Braga DA, Zandonade E, Haiter-Neto F, de-Azevedo-Vaz SL. Influence of windowing and metal artefact reduction algorithms on the volumetric dimensions of five different high-density materials: a cone-beam CT study. Dentomaxillofac Radiol 2020; 49: 20200039.
14. Jervøe-Storm PM, Hagner M, Neugebauer J, Ritter L, Zöller JE, Jepsen S, et al. Comparison of cone-beam computerized tomography and intraoral radiographs for determination of the periodontal ligament in a variable phantom. Oral Surg Oral Med Oral Pathol Oral Radiol Endod 2010; 109: e95-101.
15. AlJehani YA. Diagnostic applications of cone-beam CT for periodontal diseases. Int J Dent 2014; 2014: 865079.
16. Pauwels R, Beinsberger J, Stamatakis H, Tsiklakis K, Walker A, Bosmans H, et al. Comparison of spatial and contrast resolution for cone-beam computed tomography scanners. Oral Surg Oral Med Oral Pathol Oral Radiol 2012; 114: 127-35.
17. Huttner EA, Machado DC, de Oliveira RB, Antunes AG, Hebling E. Effects of human aging on periodontal tissues. Spec Care Dentist 2009; 29: 149-55.
18. Bartold PM. Periodontal tissues in health and disease: introduction. Periodontol 2000 2006; 40: 7-10.
19. Martins LA, Queiroz PM, Nejaim Y, Vasconcelos KF, Groppo FC, Haiter-Neto F. Evaluation of metal artefacts for two CBCT devices with a new dental arch phantom. Dentomaxillofac Radiol 2020; 49: 20190385.